Biochemical and Biophysical Research Communications 391 (2010) 874–878

Contents lists available at ScienceDirect

Biochemical and Biophysical Research Communications

journal homepage: www.elsevier.com/locate/ybbrc

Folding kinetics of recognition loop peptides from a photolyase and cryptochrome-DASH

Matthew A. Brolich, Lisa Wang, Melanie A. O'Neill *

Department of Chemistry, Simon Fraser University, Burnaby, BC, Canada V5A 1S6

ARTICLE INFO

Article history:
Received 7 November 2009
Available online 27 November 2009

Keywords:
Cryptochrome
Photolyase
Recognition loop
DNA repair
DNA base flipping
Peptide folding
Kinetics
Time-resolved fluorescence

ABSTRACT

Cryptochromes (CRY) and photolyases (PL) use a common flavin adenine dinucleotide cofactor and homologous protein scaffold to accomplish numerous, seemingly dissimilar functions. PL repairs UV-damaged DNA in a mechanism requiring light and DNA base flipping. CRY cannot repair DNA, and instead function in core biological processes including plant photomorphogenesis, circadian rhythm, and magnetoreception. One subclass, CRY-DASH, does catalyze repair of single-stranded DNA; compromised base flipping may deactivate its tight binding to duplex DNA substrates. We recently demonstrated that the a "recognition loop" involved in DNA binding by both PL and CRY-DASH is among the most flexible regions in the two proteins, and exhibits especially heightened dynamics in CRY-DASH. Here, we establish that these distinct dynamics are encoded by the loop sequences: we quantify the flexibility of the isolated loop peptides through the kinetics and activation parameters for their folding. Mirroring the dynamics within the proteins, the CRY-DASH recognition loop peptide folds 2.5-fold faster than its counterpart in PL, predominantly due to a lower enthalpy of activation. We propose that these distinct dynamics are functionally significant in DNA recognition. Binding duplex DNA in the catalytically-active base-flipped conformation imposes significant order on the recognition loop, and a corresponding entropic penalty. This may be surmounted by the more preorganized PL recognition loop, but may impose too large a barrier for the more dynamic loop in CRY-DASH. These results suggest that evolution of protein dynamics, through local sequence tuning in the recognition loop, may be an important mechanism for functional diversification in PL and CRY.

Introduction

Cryptochromes (CRY) and photolyases (PL) are a widely distributed family of flavoproteins that have evolved to perform diverse cellular tasks using highly homologous amino acid sequences and tertiary structures [1,2]. Light is used in catalysis by PL, for repair of cyclobutane pyrimidine dimers (CPD) and 6–4 photoproducts in duplex DNA, and by CRY to regulate, e.g., plant growth and development, circadian rhythm [3,4], and magnetoreception [5]. In mammals, CRY also act as light-independent transcriptional repressors in the circadian clock [3,4,6,7]. Likely common to these diverse functions are photoinduced (or ground state) electron transfer reactions mediated by the flavin adenine dinucleotide (FAD) cofactor. Catalysis by PL exploits the FAD hydroquinone/semiquinone redox couple to repair DNA with very high quantum efficiency [1]. Local tuning of FAD redox properties, in particular semiquinone stability, has recently been proposed as a central mechanism for evolution of function among CRY and PL [8].

Interaction with DNA/RNA is also expected to underlie the activity of these proteins. Catalysis by PL requires "flipping" of the damaged dinucleotide from the double helix in order to tightly bind and precisely position it for ultrafast electron transfer from its FAD cofactor [1,9,10]. Like other DNA base flipping enzymes, induced-fit binding involving reorganization of flexible loops is expected to be significant to the action of PL [11,12]. Such a "recognition loop" may be identified in PL between residues W392-P408 (Fig. 1). Structures of free and bound CPD-PL reveal loop displacement of up to 10 Å to coordinate flipping of the damaged bases from the duplex, to occupy the $\sim 10 \times 10$ Å hole left by the occluded DNA lesion, and to interact with the complementary strand (e.g., P402 and L403 with the CPD-complementary adenines) [9,13]. Movement and restructuring of this loop may contribute significantly to the barrier for DNA base flipping. Tuning of the loop dynamics may then also be an important mechanism of functional diversification in PL and CRY, in this case for regulating substrate specificity. While CRY have lost the ability to function as PL in the cell, if the barrier for base flipping is reduced, as for CPD in single stranded (ss) DNA, one subclass of CRY is capable of catalyzing repair with an efficiency similar to PL [14,15]. The CRY-DASH subclass [16–19], which shares this functional remnant of PL, is structurally very homologous to PL [13,15,16] both in global protein architecture (including its lack of a variable C-terminal extension seen in other CRY), and in FAD-binding residues. Since it

* Corresponding author. Fax: +1 778 782 3765.
E-mail address: maoneill@sfu.ca (M.A. O'Neill).

0006-291X/$ - see front matter © 2009 Elsevier Inc. All rights reserved.
doi:10.1016/j.bbrc.2009.11.155

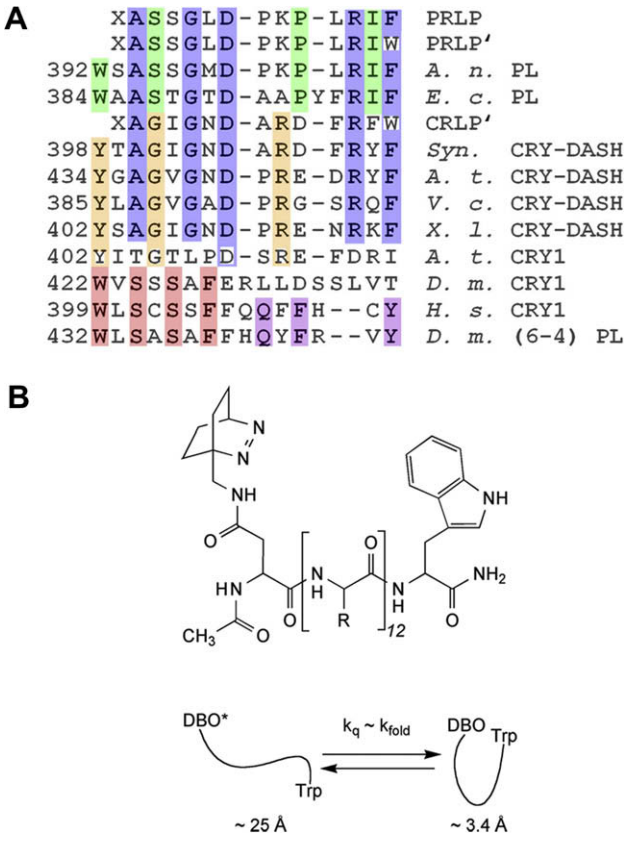

Fig. 1. (A) Sequence alignment of the recognition loop and its homologs in representative CPD-PL, CRY-DASH, plant CRY, type 1 and 2 animal CRY, and 6–4 PL; An: *A. nidulans*, Ec: *E. coli*, Syn: *Synechocystis* sp. PCC 6803, At: *A. thaliana*, Vc: *V. cholerae*, Xl: *X. laevis*, Dm: *D. melanogaster*, Hs: *H. sapiens*. Colors highlight unique residues conserved in CPD-PL (green), residues common to CPD-PL and CRY-DASH (blue), conserved in CRY-DASH (orange), and residues shared by animal CRY and 6–4 PL (pink and purple). Also shown are the sequences of PRLP, PRLP′, and CRLP′, where X = DBO-Asn. (B) Structure of the DBO-labeled peptides, where the variable R corresponds to the sequence of PRLP′ or CRLP′, and schematic of the folding experiment.

is found in all kingdoms of life, and is evolutionarily close to animal CRY [16,18], studies of CRY-DASH may shed light on the molecular origins of evolution in PL and CRY.

Using limited proteolysis, we recently revealed that the homologous "recognition loop" in CRY-DASH (Y398-I414, *Synechocystis* sp. PCC 6803, Fig. 1) is significantly more flexible than that in PL (*Anacystis nidulans* CPD-PL) [20]. We proposed that the heightened conformational dynamics in CRY-DASH may contribute to its compromised base flipping. These distinct dynamics may be rooted in conserved, local sequence variation within the recognition loops (Fig. 1), and/or be largely controlled by the protein environment. Here, to directly correlate amino acid sequence with the local tuning of recognition loop dynamics in PL and CRY-DASH, we quantitatively evaluated the folding kinetics of the isolated loop peptides (Fig. 1). These kinetics provide a direct gauge of conformational flexibility [21–25], without the influence of the protein scaffold. Our results establish that the CRY-DASH loop is intrinsically more flexible than that of PL; the CRY-DASH loop folds twice as fast, predominantly due to a lower enthalpic barrier than PL. We suggest that recognition loop sequence plays an important role in functional diversification within these proteins, and propose models for how loop flexibility impacts damaged DNA recognition.

Materials and methods

Peptide samples. All peptides were synthesized commercially (Biosyntan, Germany) following literature procedures [18]. Sequences were confirmed by MALDI-TOF mass spectrometry, and purity (>95%) was established by HPLC. Peptide samples (typically ~65 μM) were prepared in aerated phosphate buffer (10 mM KH_2PO_4/K_2HPO_4, 150 mM NaCl, pH 7.5), or 8 M urea, and concentrations verified by UV–vis spectroscopy (ε_{280} = 5500 M^{-1} cm^{-1} for single Trp peptides).

Fluorescence spectroscopy. Fluorescence data was acquired using a Horiba-JobinYvon Fluorolog 3 spectrometer equipped with double excitation and emission monochromators, a cooled photomultiplier detector (IBH), and electronics for time-correlated single photon counting (TCSPC). A 450 W xenon-arc lamp was used as a light-source for steady-state experiments. Emission spectra were acquired by exciting Trp at 295 nm (⩽2 nm bandpass), or DBO at 430 nm (⩽8 nm bandpass), and corrected for the instrument response and buffer scattering. For TCSPC experiments on DBO, the excitation source was a 375 nm laser diode (~70 ps FWHM) operating at 100 kHz repetition rate (forward mode, 500 ns/1 μs/2 μs total time binned into 2048 channels). Emission was passed through a double monochromator with a 10–15 nm bandpass centered at 430 nm. Fluorescence decays were collected until at least 10,000 counts accumulated in the peak channel. Sample temperature was maintained (±0.1 °C) using a Peltier-controlled thermostated sample holder.

Most DBO* intensity versus time profiles were fit to a single exponential decay (with or without reconvolution with the instrument response function yielded the same lifetimes). Under native conditions, the decays of DBO in PRLP′ and CRLP′ were better modeled by a double first-order exponential expression to yield a major, faster decaying component (85–90%), and a minor, slower decay component. Since this minor component was detected only for the Trp-terminated peptides, and was eliminated by denaturant, it is not likely a fluorescence artifact or impurity. The reported rate constants under native conditions are the amplitude-weighted averages of the two components.

Results and discussion

Experimental design

End-to-end contact formation (folding) is a direct gauge of peptide flexibility [21–25]. Such peptide folding dynamics are readily probed by time-resolved fluorescence for peptides possessing Trp and 2,3-diazabicyclo[2.2.2]oct-2-ene (DBO) at opposite termini (Fig. 1) [26–32]. Since the absorption and emission of DBO and Trp are well separated, each may be selectively excited: quenching of Trp* by FRET to DBO provides information on donor–acceptor distances in the 5–20 Å regime [30], while diffusion-controlled quenching of the long-lived DBO* ($\tau \sim 325$ ns in water) upon contact with Trp reports on folding rate constants in the 10^6–10^7 s^{-1} range expected for short peptides (~5–15-mers) [26–32]. These rate constants may be directly evaluated from the quenching kinetics, Eq. (1), where τ and τ_o are the DBO* fluorescence lifetimes in a peptide with and without a terminal Trp, respectively [26–32].

$$k_q = 1/\tau - 1/\tau_o = k_{\text{fold}} \quad (1)$$

Aside from weak, activated quenching by Cys, Met, and Tyr, DBO* is unreactive towards other amino acids [27].

Here, we probe folding of PL (*A. nidulans*) and CRY-DASH (*Synechocystis* sp. PCC 6803) recognition loop peptides, PRLP and CRLP, respectively. In our peptides (Fig. 1), the loop N-terminal W/Y has been removed, and the adjacent residue replaced by a DBO-modified Asn. The C-terminal residue is either the loop-intrinsic Phe in PRLP, which is the quencher-free peptide used for evaluation of τ_o, or Trp, for measurement of τ in PRLP′ and CRLP′. Conservative replacement of a loop Met by Leu in PRLP/PRLP′, and a loop Tyr by Phe in CRLP′, ensure that the terminal Trp is the only quencher in each peptide sequence.

Folding kinetics of the recognition loop peptides

The fluorescence decay of DBO* in PRLP, which lacks a Trp quencher, is single exponential with a lifetime of 241 ± 5 ns in aerated phosphate buffer (pH 7.5) at 20 °C (Fig. 2A). This is somewhat shorter than the lifetime of free DBO* measured under the same conditions (323 ± 5 ns), but within the range (360–227 ns) found for DBO* conjugated to peptides lacking Trp, or the other weak quenchers (Tyr, Met, Cys) [32]. The shorter DBO* lifetime within control peptides is not likely due to amino acid quenching, since the second-order rate constants for reaction of DBO* with Phe and His are 6–8 $\times$ 10^6 M^{-1} s^{-1}, and those of the other 14 amino acids are <10^6 M^{-1} s^{-1} (cf. 2 $\times$ 10^9 M^{-1} s^{-1} for Trp) [27]. It may instead be related to the nature of the covalent attachment, or environment at the N/C-terminus where the DBO is coupled. As expected, PRLP′ and CRLP′ have significantly shorter lifetimes of 92 ± 3 and 47 ± 2 ns, respectively, that are 75–90% quenched relative to DBO*, and 65–80% less than PRLP (Fig. 2A). Intermolecular quenching is not anticipated at our peptide concentrations [27–32]. Moreover, we find the lifetime of DBO* to be independent of peptide concentration (50–100 μM), and have ruled out an intermolecular quenching mechanism in experiments with mixed samples of PRLP and unlabeled PRLP′. Quenching of DBO* in PRLP′ and CRLP′ is intramolecular, due to folding and contact with the C-terminal Trp. Significantly, folding kinetics evaluated from Eq. (1) reveal that CRLP′ (k_{fold} = 17.2 $\times$ 10^6 s^{-1}) folds 2.5-fold faster than PRLP′ (k_{fold} = 6.8 $\times$ 10^6 s^{-1}). The standard deviations on these k_{fold} values are <10%.

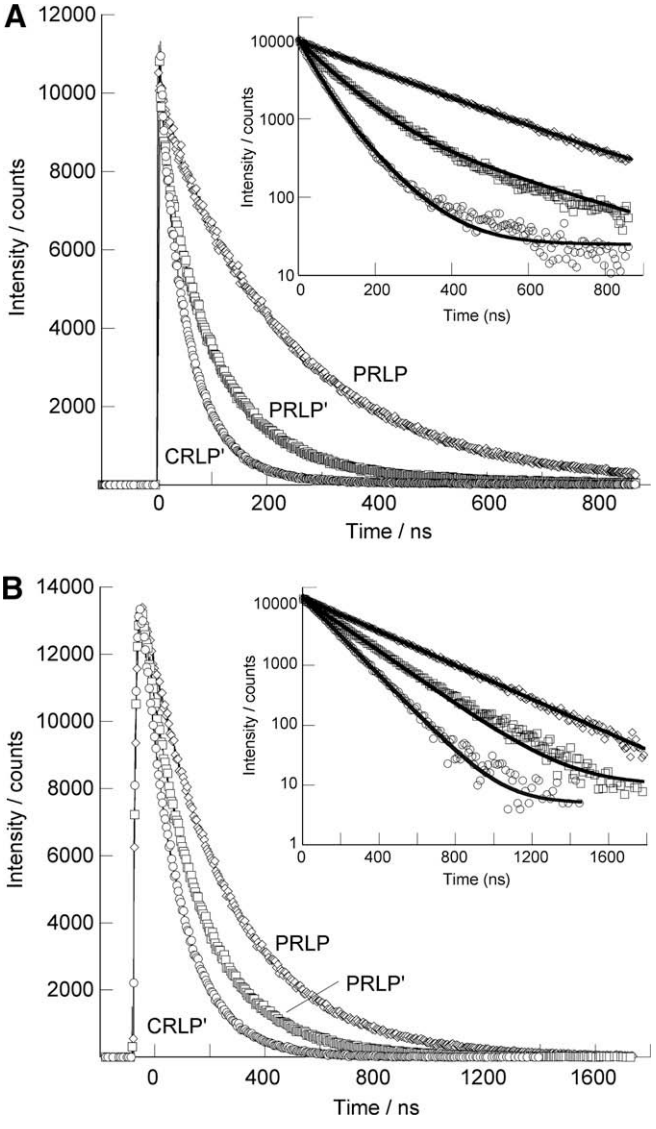

Fig. 2. Fluorescence decays (λ_{ex} = 372 nm, λ_{em} = 430 nm) of DBO-labeled recognition loop peptides (~65 μM) in aerated phosphate buffer, pH 7.5 (A), or in 8 M urea (B) at 20 °C. The insets show the decays on a semi-logarithmic scale, where the solid line is the fit of experimental data to a single or double first-order exponential decay (see text). Only 10–20% of data is shown in order to visualize the fit lines.

As is evident in Fig. 2A, unlike PRLP, the decay kinetics of PRLP′ and CRLP′ are not completely monoexponential. The reported lifetimes are the amplitude-weighted averages from fits of the experimental data to a double first-order exponential decay. The data is well fit to this expression (Fig. 2A, inset), yielding lifetimes τ_F = 85 ns (90%)/τ_s = 303 ns (10%) for PRLP′ and τ_F = 44 ns (85%)/τ_s = 110 ns (15%) for CRLP′ at 20 °C. Multiexponential peptide folding kinetics have been ascribed to incomplete conformational averaging [24,31]: intrachain interactions have been detected even for highly flexible, "unstructured" peptides lacking hydrophobic groups [25]. Only if these conformers interconvert rapidly, relative to the folding timescale, and the equilibrium population of folded conformers is small, are single exponential folding kinetics expected [21,22,27–29].

To address this possible explanation for the double exponential decay of DBO* in PRLP′ and CRLP′, we first evaluated their average end-to-end distances from the efficiency of FRET between Trp* and DBO [30]. FRET quenching of Trp* is clearly evident by the enhanced Trp emission in non-DBO-labeled peptides (Fig. S1), and sensitized emission of DBO, seen as a long lifetime component at 430 nm following selective excitation of Trp at 295 nm (Fig. S2). The FRET efficiencies evaluated from steady-state or time-resolved measurements are comparable (±5%), and both are higher for CRLP′ (E = 0.4) than PRLP′ (E = 0.1). Given an R_o of 10 Å for the Trp*/DBO pair [30], we calculate an average end-to-end distance of ~11 and 15 Å for CRLP′ and PRLP′, respectively (cf. ~25 Å estimated for the fully extended peptide).

These FRET efficiencies suggest differences in the ensemble-averaged distribution of structures in CRLP′ and PRLP′. Consequently, we examined the peptides under denaturing conditions. The decay of DBO* in each of the three peptides is monoexponential in 8 M urea; the minor decay component detected for CRLP′ and PRLP′ under native conditions may indeed reflect population of more than one structure in slow exchange. The DBO* fluorescence lifetimes of PRLP, PRLP′, and CRLP′ increase to 304, 188, and 122 (±2) ns, respectively, under denaturing conditions at 20 °C. This is expected for PRLP, since increased viscosity should enhance the intrinsic fluorescence lifetime. The increased viscosity may exert several effects on the folding kinetics. It is expected to slow end-to-end collision; however, by disrupting intrachain interactions, the denaturant may also increase both peptide flexibility and end-to-end distance [25]. The net effect, seen here, and with other peptides [20,25], is slower folding. Importantly, the difference in k_{fold} is maintained for the two peptides, even when any persistent intrachain interactions are lost. In 8 M urea, k_{fold} = 2.0 and 4.9 $\times$ 10^6 s^{-1} for PRLP′, and CRLP′, respectively. The close match in relative reactivity under native and denaturing conditions confirms that the quenching rate constants report on peptide folding kinetics and conformational flexibility [20].

The folding kinetics of loop peptides from PL and CRY-DASH are consistent with those for designed peptides of similar length. For instance, k_{fold} for the DBO-labeled 16-mer, Trp-(Gly-Ser)$_6$-DBO-NH_2 is 2.0 $\times$ 10^7 s^{-1} at 23 °C [27], nearly identical to that of CRLP′ under similar conditions. The 2.5-fold difference in the folding kinetics between the mixed-sequence PRLP′ and CRLP′ is significant: the maximum sequence variation in folding kinetics, seen for DBO-X_6-Trp homopeptides (excluding polyprolines), is ~1 or-

der of magnitude: k_{fold} is $39 \times 10^6\ s^{-1}$ for X = Gly, and $2–4 \times 10^6\ s^{-1}$ for X = Lys/Val/Ile [28], and single amino acid substitutions within similar sized peptides alter folding rate constants by ~1.1- to 6-fold [22,29]. The finding that the combination of residues in CRLP′ is more dynamic than that in PRLP′ is also important: of the 12 intervening residues in CRLP′ and PRLP′ (Fig. 1), 4 are matched and conserved between CPD-PL and CRY-DASH. Notably different are a conserved Gly in CRY-DASH, replaced by Ser in CPD-PL, and a conserved Pro in CPD-PL, lost in CRY-DASH. Gly and Pro are expected to exert a large influence on peptide dynamics, and to be important in early stages of folding [24]. Yet, while PRLP may possesses more rigidifying residues, based on a scale for individual amino acids [20], the flexibility of these residues necessarily depends on sequence context [24], and their contribution to dynamics of natural peptides is not readily predicted. Our quantification of the folding kinetics indicates that CRLP′ is intrinsically more flexible than PRLP′. These results provide a rationale, at the primary sequence level, for the heightened conformational dynamics of this loop in CRY-DASH, and its more restricted movement in PL (Fig. 3) [20].

Activation parameters for recognition loop folding

To investigate the origin of these distinct conformational dynamics, we measured the activation parameters for folding under native and denaturing conditions. While the lifetime of PRLP increases weakly with decreasing temperature from 55 to 5 °C [29], that of PRLP′ and CRLP′ increases significantly, and the k_{fold} values decrease by ~5-fold (Table S1). The Eyring plots (Fig. 4) yield apparent activation free enthalpies between ~20 and 23 kJ mol^{-1} (Table 1). As in other variable-temperature folding studies of DBO-peptides [29,31], the activation parameters have not been corrected for (yet unknown) contributions from changes in viscosity [24]. The magnitudes of these values, comparable to previous reports for peptide folding, indicate that both solvent friction and internal friction contribute to the activation barriers for folding [24,29,31]. Increased solvent friction in the more viscous urea may contribute to greater folding barriers under denaturing conditions [29]. The greater internal friction of PRLP′ is evident by its higher free energy of activation in both buffer and urea (Table 1). The loss in conformational entropy is nearly the same for folding of CRLP′ and PRLP′; the height of the enthalpic barrier dominates the difference in folding kinetics. This matches folding of $(Ser)_n$-X-$(Ser)_n$ peptides, where X = Gly decreased the enthalpic barrier, while X = Pro increased it, each with little effect on folding entropy [24].

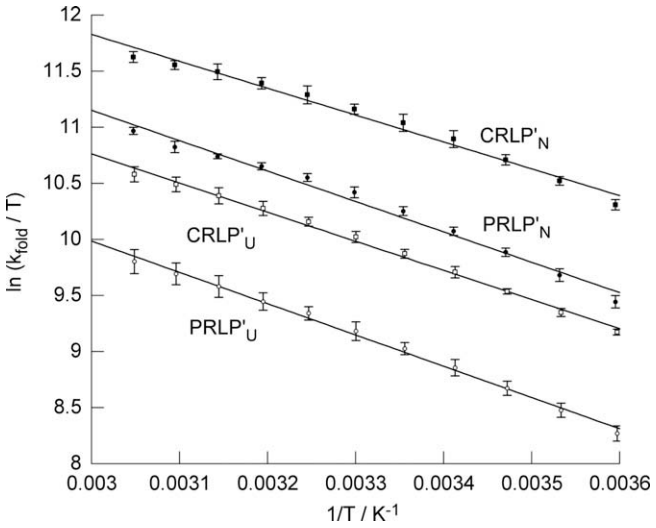

Fig. 4. Eyring plots of the temperature-dependent folding rate constants for the recognition loop peptides under native (N, phosphate buffer pH 7.5), or denaturing (U, 8 M urea) conditions. Data points are averages of four experiments with standard deviation shown. Lines are fits to the Erying equation: $\ln(k_{fold}/T) = -\Delta H^{\ddagger}/R(1/T) + \ln k_B/h + \Delta S^{\ddagger}/R$.

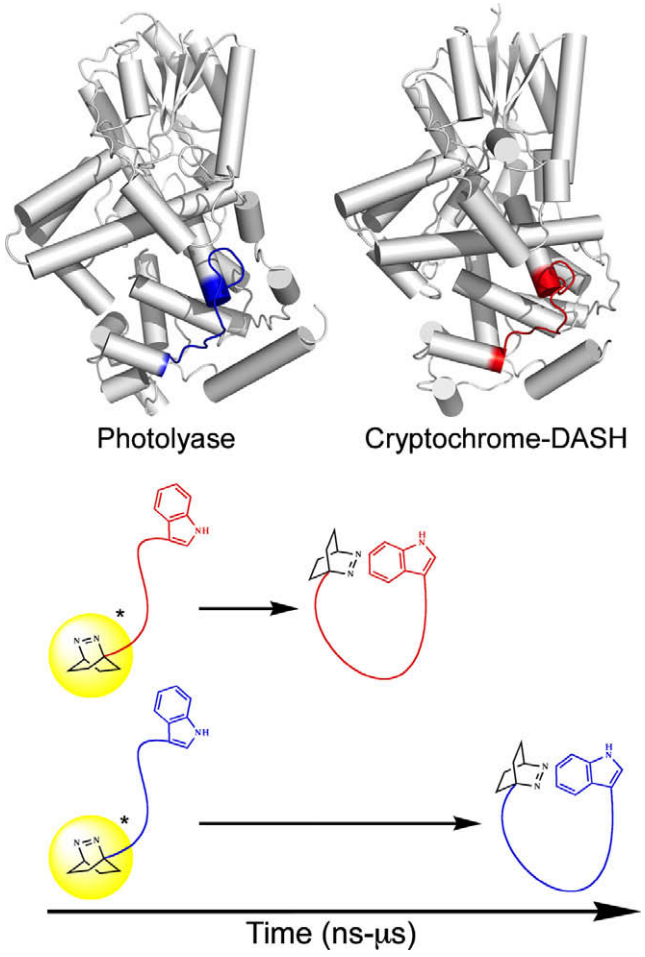

Fig. 3. Crystal structures (rendered in Pymol using pdb files 1qnf [13] and 1np7 [16]) highlighting the recognition loop in PL (blue) and CRY-DASH (red), and schematic of the peptide folding results. These results demonstrate that the heightened loop dynamics observed in CRY-DASH are rooted in differences in loop sequence.

Functional implications of recognition loop dynamics

Peptide folding kinetics reveal that the sequence of the CRY-DASH recognition loop confers enhanced flexibility, relative to its counterpart in PL, predominantly by lowering the enthalpic barrier to conformational rearrangement. These sequence-encoded dynamics are maintained within the proteins, where the loop dynamics are seen to be enhanced in CRY-DASH (Fig. 3) [20]. The

Table 1
Activation parameters for peptide folding.[a]

	Native			Denaturing		
	$\Delta G^{\ddagger}$[b]	$\Delta H^{\ddagger}$	$T\Delta S^{\ddagger}$[b]	$\Delta G^{\ddagger}$[b]	$\Delta H^{\ddagger}$	$T\Delta S^{\ddagger}$[b]
CRLP′	31.5	19.9 ± 0.1	−11.6 ± 0.2	34.3	21.3 ± 0.3	−13.0 ± 0.4
PRLP′	33.4	22.5 ± 0.4	−10.9 ± 0.4	36.4	23.3 ± 0.4	−13.1 ± 0.3

[a] Averages and standard errors of four trials in kJ mol^{-1}; error on $\Delta G^{\ddagger} \leqslant \pm 0.5$.
[b] Evaluated at 20 °C.

larger barrier to conformational rearrangement in PL may encode more preorganization of its recognition loop in the absence of substrate. This may reduce the entropic penalty associated with binding duplex DNA: in complex with substrate, the loop is ordered by insertion within the duplex, and interaction with the complementary strand, in place of the occluded damaged dinucleotide [9]. The less preorganized recognition loop of CRY-DASH may render this entropic penalty too high, thereby compromising its ability to bind double-stranded DNA in the catalytically-competent, base-flipped conformation. Consistent with this proposal is the fact that CRY-DASH tightly binds and efficiently repairs CPD in single-stranded regions of DNA [14,15], where this entropic penalty is expected to be reduced.

Selective repair of CPD in single-stranded DNA is unique to CRY-DASH [14]: PL repairs single- and double-stranded DNA substrates with comparable efficiency, and other subclasses of CRY show no activity with any CPD-containing DNA. While the latter likely reflects some defects in the catalytic chemistry, differences in recognition loop sequence among PL and CRY (Fig. 1) point to an important role for its tuning of substrate specificity. For instance, structures of PL and CRY-DASH bound to single- [15] and double-stranded [9] DNA, respectively, reveal that common loop residues D399 and R404 (*A. nidulans* PL numbering) may recognize the CPD or damaged strand. Neither of these residues are conserved in plant or animal CRY, or 6–4 PL. Loop residues A394, G399, and F406 are similarly unique to PL and CRY-DASH. These are more distal from the CPD, but may play a defining role in loop dynamics. In combination with other PL-specific loop residues, these may tune the balance between the flexibility required for DNA base flipping, and the preorganization needed to minimize entropic barriers. In CRY-DASH this balance has been tipped, since base flipping is compromised, although aspects of CPD recognition remain. The corresponding loops in other CRY show significant homology with each other, but differ more significantly from CPD-PL. Their functional divergence may involve both loss of both base flipping, and CPD recognition. In this regard, the homology between recognition loops in animal CRY, especially type 2 animal CRY (e.g., human), and 6–4 PL is interesting, since 6–4 PL retain base flipping activity, but for a distinct DNA substrate [10]. Evolution of loop sequence likely plays a key role in functional diversification of PL and CRY, through tuning of substrate recognition.

Acknowledgments

The authors thank the Natural Sciences and Engineering Research Council of Canada and the Michael Smith Foundation for Health Research for financial support, and Prof. W.M. Nau for facilitating our acquisition of DBO-labeled peptides.

Appendix A. Supplementary data

Supplementary data associated with this article can be found, in the online version, at doi:10.1016/j.bbrc.2009.11.155.

References

[1] A. Sancar, Structure and function of DNA photolyase and cryptochrome blue-light photoreceptors, Chem. Rev. 103 (2003) 2203–2237.
[2] L.O. Essen, T. Klar, Light-driven DNA repair by photolyases, Cell. Mol. Life Sci. 63 (2006) 1266–1277.
[3] A.R. Cashmore, Cryptochromes: enabling plants and animals to determine circadian time, Cell 114 (2003) 537–543.
[4] P. Emery, W.V. So, M. Kaneko, J.C. Hall, M. Robash, P. Emery, CRY, a *Drosophila* clock and light-regulated cryptochrome, is a major contributor to circadian rhythm resetting and photosensitivity, Cell 95 (1998) 669–679.
[5] R.J. Gegear, A. Casselman, S. Waddell, S.M. Reppert, Cryptochrome mediates light-dependent magnetosensitivity in *Drosophila*, Nature 454 (2008) 1014–1018.
[6] Q. Yuan, D. Metterville, A.D. Briscoe, S.M. Reppert, Insect cryptochromes: gene duplication and loss define diverse ways to construct insect circadian clocks, Mol. Biol. Evol. 24 (2007) 948–955.
[7] A. Sancar, Regulation of the mammalian circadian clock by cryptochrome, J. Biol. Chem. 279 (2004) 34079–34082.
[8] K. Hitomi, L. DiTacchio, A.S. Arvai, J. Yamomoto, S.-T. Kim, T. Todo, J.A. Tainer, S. Iwai, S. Panda, E.D. Getzoff, Functional motifs in the (6–4) photolyase crystal structure make a comparative framework for DNA repair photolyases and clock cryptochromes, Proc. Natl. Acad. Sci. USA 106 (2009) 6962–6967.
[9] A. Mees, T. Klar, P. Gnau, U. Hennecke, A.P.M. Eker, T. Carell, L.-O. Essen, Crystal structure of a photolyase bound to a CPD-Like DNA lesion after in situ repair, Science 306 (2004) 1789–1793.
[10] M.J. Maul, T.R.M. Barends, A.F. Glas, M.J. Cryle, T. Domratcheva, S. Schneider, I. Schlichting, T. Carell, Crystal structure and mechanism of a DNA (6–4) photolyase, Angew. Chem. Int. Ed. 47 (2008) 10076–10086.
[11] R.A. Estabrook, N. Reich, Observing an induced-fit mechanism during sequence-specific DNA methylation, J. Biol. Chem. 281 (2006) 37205–37214.
[12] J.T. Stivers, Site-specific DNA damage recognition by enzyme-induced base flipping, Prog. Nucl. Acids Res. Mol. Biol. 77 (2004) 37–65.
[13] T. Tamada, K. Kitadokoro, Y. Higuchi, K. Inaka, A. Yasui, P.E. deRuiter, A.P.M. Eker, K. Miki, Crystal structure of DNA photolyase from *Anacystis nidulans*, Nat. Struct. Biol. 4 (1997) 887–891.
[14] C.P. Selby, A. Sancar, A cryptochrome/photolyase class of enzymes with single-stranded DNA-specific photolyase activity, Proc. Natl. Acad. Sci. USA 103 (2006) 17696–17700.
[15] R. Pokorny, T. Klar, U. Hennecke, T. Carell, A. Batschauer, L.-O. Essen, Recognition and repair of UV lesions in loop structures of duplex DNA by DASH-type cryptochrome, Proc. Natl. Acad. Sci. USA 105 (2008) 21023–21027.
[16] R. Brudler, K. Hitomi, H. Daiyasu, H. Toh, K. Kucho, M. Ishiura, M. Kanehisa, V.A. Roberts, T. Todo, J.A. Tainer, E.D. Getzoff, Identification of a new cryptochrome class: structure, function, and evolution, Mol. Cell 11 (2003) 59–67.
[17] K. Hitomi, K. Okamoto, H. Daiyasu, H. Miyashita, S. Iwai, H. Toh, M. Ishiura, T. Todo, Bacterial cryptochrome and photolyases: characterization of two photolyases-like genes of *Synechocystis* sp. PCC6803, Nucleic Acids Res. 28 (2000) 2353–2362.
[18] H. Daiyasu, T. Ishikawa, K.-I. Kuma, S. Iwai, T. Todo, H. Toh, Identification of cryptochrome DASH from vertebrates, Genes Cells 9 (2004) 479–495.
[19] K. Zikihara, T. Ishikawa, T. Todo, S. Tokutomi, Involvement of electron transfer in the photoreaction of zebrafish cryptochrome-DASH, Photochem. Photobiol. 84 (2008) 1016–1023.
[20] N.R. McLeod, M.A. Brolich, M.J. Damiani, M.A. O'Neill, Distinct recognition loop dynamics in cryptochrome-DASH and photolyase revealed by limited proteolysis, Biochem. Biophys. Res. Commun. 385 (2009) 424–429.
[21] O. Bieri, J. Wirz, B. Hellrung, M. Schutkowski, M. Drewello, T. Kiefhaber, The speed limit for protein folding measured by triplet–triplet energy transfer, Proc. Natl. Acad. Sci. 96 (1999) 9597–9601.
[22] F. Krieger, B. Fierz, O. Bieri, M. Drewello, T. Kiefhaber, Dynamics of unfolded polypeptide chains as model for the earliest steps in protein folding, J. Mol. Biol. 332 (2003) 265–274.
[23] F. Kreiger, B. Fierz, F. Axthelm, K. Joder, D. Meyer, T. Kiefhaber, Intrachain diffusion in a protein loop fragment from carp parvalbumin, Chem. Phys. 307 (2004) 209–215.
[24] F. Krieger, A. Möglich, T. Keifhaber, Effect of proline and glycine residues on dynamics and barriers of loop formation in polypeptide chains, J. Am. Chem. Soc. 127 (2005) 3346–3352.
[25] A. Möglich, K. Joder, T. Kiefhaber, End-to-end distance distributions and intrachain diffusion constants in unfolded polypeptide chains indicate intramolecular hydrogen bond formation, Proc. Natl. Acad. Sci. USA 103 (2006) 12394–12399.
[26] F. Huang, W.M. Nau, Photochemical techniques for studying the flexibility of polypeptides, Res. Chem. Intermed. 31 (2005) 717–726.
[27] R.R. Hudgins, F. Huang, G. Gramlich, W.N. Nau, A fluorescence-based method for direct measurement of submicrosecond intramolecular contact formation in biopolymers: an exploratory study with polypeptides, J. Am. Chem. Soc. 124 (2002) 556–564.
[28] F. Huang, W.M. Nau, A conformation flexibility scale for amino acids in peptides, Angew. Chem. Int. Ed. 42 (2003) 2269–2272.
[29] F. Huang, R.R. Hudgins, W.M. Nau, Primary and secondary structure dependence of peptide flexibility assessed by fluorescence-based measurement of end-to-end collision rates, J. Am. Chem. Soc. 126 (2004) 16665–16675.
[30] H. Sahoo, D. Roccatano, M. Zacharias, W.M. Nau, Distance distributions of short polypeptides recovered by fluorescence resonance energy transfer in the 10 Å domain, J. Am. Chem. Soc. 128 (2006) 8118–8119.
[31] D. Roccatano, H. Saboo, M. Zacharias, W.M. Nau, Temperature dependence of looping rates in a short peptide, J. Phys. Chem. B 111 (2007) 2639–2646.
[32] A. Henning, M. Florea, D. Roth, T. Enderle, W.M. Nau, Design of peptide substrates for nanosecond time-resolved fluorescence assays of proteases: 2,3-diazabicyclo[2.2.2]oct-2-ene as a noninvasive fluorophore, Anal. Biochem. 360 (2007) 255–265.